AMERICAN SOCIETY FOR MICROBIOLOGY | Molecular and Cellular Biology®

RESEARCH ARTICLE

Endogenous Telomerase Reverse Transcriptase N-Terminal Tagging Affects Human Telomerase Function at Telomeres *In Vivo*

Kunitoshi Chiba, Jacob M. Vogan, Robert A. Wu, Manraj S. Gill, Xiaozhu Zhang, Kathleen Collins, Dirk Hockemeyer

Department of Molecular and Cell Biology, University of California, Berkeley, Berkeley, California, USA

ABSTRACT Telomerase action at telomeres is essential for the immortal phenotype of stem cells and the aberrant proliferative potential of cancer cells. Insufficient telomere maintenance can cause stem cell and tissue failure syndromes, while increased telomerase levels are associated with tumorigenesis. Both pathologies can arise from only small perturbation of telomerase function. To analyze telomerase at its low endogenous expression level, we genetically engineered human pluripotent stem cells (hPSCs) to express various N-terminal fusion proteins of the telomerase reverse transcriptase from its endogenous locus. Using this approach, we found that these modifications can perturb telomerase function in hPSCs and cancer cells, resulting in telomere length defects. Biochemical analysis suggests that this defect is multileveled, including changes in expression and activity. These findings highlight the unknown complexity of telomerase structural requirements for expression and function *in vivo*.

KEYWORDS genome editing, telomerase, telomeres, pluripotent stem cells, CRISPR/Cas9, embryonic stem cells

Received 1 October 2016 **Returned for modification** 2 November 2016 **Accepted** 15 November 2016

Accepted manuscript posted online 21 November 2016

Citation Chiba K, Vogan JM, Wu RA, Gill MS, Zhang X, Collins K, Hockemeyer D. 2017. Endogenous telomerase reverse transcriptase N-terminal tagging affects human telomerase function at telomeres *in vivo*. Mol Cell Biol 37:e00541-16. https://doi.org/10.1128/MCB.00541-16.

Address correspondence to Dirk Hockemeyer, hockemeyer@berkeley.edu.

Telomerase is a reverse transcriptase that synthesizes *de novo* telomeric repeats, which have the sequence 5′-TTAGGG-3′ in vertebrates, and thereby maintains telomeres (1, 2). Its enzymatic activity counteracts terminal sequence loss from linear chromosomes and ensures the long-term proliferative capacity of human stem cells (3). When aberrantly active, telomerase expression can grant the immortal phenotype of human cancer cells (4). The minimal components for catalytic activity reconstitution are the protein component telomerase reverse transcriptase (TERT) and the noncoding telomerase RNA (TR), which bears the template region to synthesize telomeric repeats. Telomerase is expressed at low levels in stem cells and cancer cells. Estimates of the numbers of functional RNPs that are generated from 2 to 20 copies of TERT mRNA per cell range from 50 to a few hundred (5–8). Under these conditions, telomerase can be in substoichiometric abundance in relation to the number of telomeres that are present after DNA replication. Telomerase is not generally present at telomeres but is actively recruited during the S phase to a subset of telomeres through protein-protein interactions that occur between telomerase and the telomere. This interaction is mediated by the N-terminal domain of TERT, called the TEN domain (telomerase essential N-terminal domain) (9), and the telomere by the shelterin complex, a six-member protein complex (10). Specifically, a small region in the shelterin protein TPP1 called the TEL patch interacts with the telomerase TEN domain (11–18). This interaction is essential for telomere maintenance, as cells genetically engineered to lack an acidic loop within the TEL patch phenocopy telomerase knockout cells (18). Furthermore, residue swap experiments that exchange critical amino acids in the TEN domain and

the TEL patch indicate a direct interaction between TERT and TPP1 (19). Beyond telomerase recruitment, TPP1, together with its shelterin interacting partner POT1, can have additional activating and inhibitory roles in telomerase action at telomeres, as reviewed in references 20 and 21.

TPP1 binds to the telomere through its interaction with TIN2, which itself binds to the double-stranded telomeric binding proteins TRF1 and TRF2 (22). In addition, TPP1 recruits the single-stranded binding protein POT1 to telomeres (23, 24). Perturbation of the shelterin protein-interaction network by overexpression or loss of function results in telomere length changes in human cells (24–29). However, how these proteins function in cells in which telomere length is at homeostasis is not well understood. At telomere homeostasis, telomere shortening caused by nucleolytic degradation and by the end replication problem is at equilibrium with telomere elongation. Yet telomeres at different chromosome ends within one cell or telomeres of the same chromosome within a cell population can differ in length. Previous experiments suggested that overall telomere length homeostasis is established by a process that stochastically elongates shorter telomeres preferentially over long telomeres (reviewed in reference 20). The underlying counting mechanism that distinguishes telomeres of different lengths and communicates the information to telomerase is currently not well understood (20, 30).

Several lines of evidence indicate that telomerase, particularly, the process of telomerase recruitment to individual telomeres, must be studied in the context of the physiological expression levels regulated within the endogenous genetic context. Importantly, overexpression of telomerase in human cells leads to the rapid telomere elongation that has been suggested to be unrestrained and not subject to the regulatory mechanisms that establish telomere homeostasis (31). This excessive action of telomerase at telomeres suggests that overexpression of telomerase can bypass the transient nature of telomerase localization to telomeres; when overexpressed, several TERT molecules constitutively localize to most telomeres within a cell, which is not observed in naturally telomerase-positive cells (12).

Until recently, direct observation of telomerase action at telomeres without overexpression has been considerably hampered by the lack of a reliable antibody detecting endogenous levels of TERT. In fixed cells, fluorescence *in situ* hybridization (FISH) for examination of the telomerase RNA or the localization of Cajal bodies to telomeres has been used as a proxy for the localization of TERT to telomeres (32, 33). However, recent genetic data suggest that these associations might not be directly reporting on telomerase action at telomeres (34–36). With the advent of genome editing in human pluripotent stem cells (reviewed in reference 37), an experimental system became available that can overcome these challenges. Robust protocols to genetically modify human embryonic stem cells (hESCs) and induced pluripotent stem cells (iPSCs) (37–41), collectively referred to as hPSCs, have recently become available. With these technical developments, epitope tags or fluorescent reporter genes can now be inserted into the hPSC genome to endogenously mark cells for imaging or biochemical purification.

hPSCs are an ideal model system to study telomerase regulation, as they are telomerase positive (42, 43) but can be rapidly differentiated into telomerase-negative cells. Moreover, the reverse process of telomerase reactivation can be studied during the reprogramming of somatic cells into iPSCs (44–46). Due to their constitutive telomerase expression, hPSCs are immortal. However, in contrast to tumor cells, they have functional DNA surveillance and cell cycle checkpoints and therefore are well suited to the study of the effects of telomere length regulation and dysfunction on these pathways.

Here, we report on the analysis of genetically engineered hPSCs that express TERT with a variety of N-terminal fusions from the endogenous locus. We chose to modify the N terminus instead of the C terminus of TERT because the addition of a hemagglutinin (HA) tag at the C terminus of TERT results in a striking defect in telomere maintenance despite almost wild-type enzymatic activity *in vitro* (47). Interestingly,

separation-of-function mutants in TERT, termed DAT mutants, that retain catalytic activity but fail to immortalize human primary fibroblasts have been identified at both the C terminus and in the N-terminal TEN domain (47–50). The N-terminal DAT mutants alter residues subsequently identified as part of the interaction interface with TPP1 required for localization and activity of telomerase at telomeres (18, 19, 33). Mutations near the N terminus can also have pronounced defects with effects on TERT's ability to sequentially add multiple telomeric repeats without dissociating from the telomere, a specialized feature of telomerase called repeat addition processivity (RAP) (51).

We employed a genome-editing strategy to tag TERT endogenously at its N terminus based on a protocol that we had previously established to genetically engineer hPSCs to carry mutations in the TERT promoter (52). This protocol was developed to engineer hPSCs that carry mutations in the TERT promoter, representing the most frequent noncoding mutations in human cancer as reviewed in reference 53. Here, we have extended this targeting strategy to test several N-terminal modifications of TERT with the goal of directly tagging TERT in hPSCs to increase the ease of performing immunofluorescence and biochemical experiments.

Unexpectedly, we observed significant changes in telomerase biology as a result of N-terminal tagging during these experiments. We demonstrated that most N-terminal fusion proteins generated by inserting sequences at the translational start site of TERT show a pronounced defect in telomerase action at telomeres and result in reduced telomere length. Biochemical and cellular assays suggest that this defect is multifactorial, indicating that much remains to be learned about the cellular mechanisms for regulation of telomerase action at telomeres.

RESULTS

Endogenous epitope tagging of TERT using genome editing. To understand the regulation of TERT in living cells, we engineered the endogenous TERT locus in hESCs to carry a Halo tag (54) at the N terminus (Halo-TERT hESCs). A Halo tag covalently binds to its synthetic ligands conjugated with fluorescent dyes such as tetramethylrhodamine (TMR). We chose this strategy over conventional green fluorescent protein (GFP) tagging as it is expected to result in more highly photostable and brighter fluorescently marked proteins and thereby facilitates single-molecule imaging. To establish hESC lines with TERT tagged at the N terminus, we modified the two-step, scarless genome editing of the TERT locus that we previously reported (52) (Fig. 1A). First, the region between bp −1462 and +67 relative to the translational start site (ATG) of the TERT gene was deleted using two single-guide RNAs (sgRNA). Cells homozygous for this deletion ($TERT^{\Delta/\Delta}$) lacked TERT expression and, consequently, telomerase activity. As a result, these cells showed progressive telomere shortening and died about 150 days after the deletion event (18). However, in cells that were subjected to a second targeting step that reintroduced the deleted element, telomerase activity and cellular viability were restored and telomeres reverted to the wild-type length over time. This second editing step was conducted using a specific sgRNA against the new junction (−1462 to +67) to reinsert into the deleted region either the wild-type sequence or sequences that insert a tag after the first ATG (Fig. 1A). After the second targeting, targeted cells restore TERT expression and are gradually enriched whereas untargeted parental $TERT^{\Delta/\Delta}$ hESCs die at around 150 days (Fig. 1B).

Initially, we focused on generating cells that expressed an N-terminal Halo-tag-targeted TERT from the endogenous locus. We successfully generated Halo-TERT-expressing cells that proliferated beyond the proliferative capacity of $TERT^{\Delta/\Delta}$ cells (data not shown). However, direct comparison of Halo-TERT and isogenic wild-type (wt) cells, in which we introduced the wild-type sequence without the tag, revealed a striking proliferation defect of Halo-TERT hESCs. Halo-TERT cells had reduced colony size and showed cell morphology associated with dysfunctional telomerase in hESCs (18). The proliferation and viability of these cultures were impacted too severely to permit further characterization.

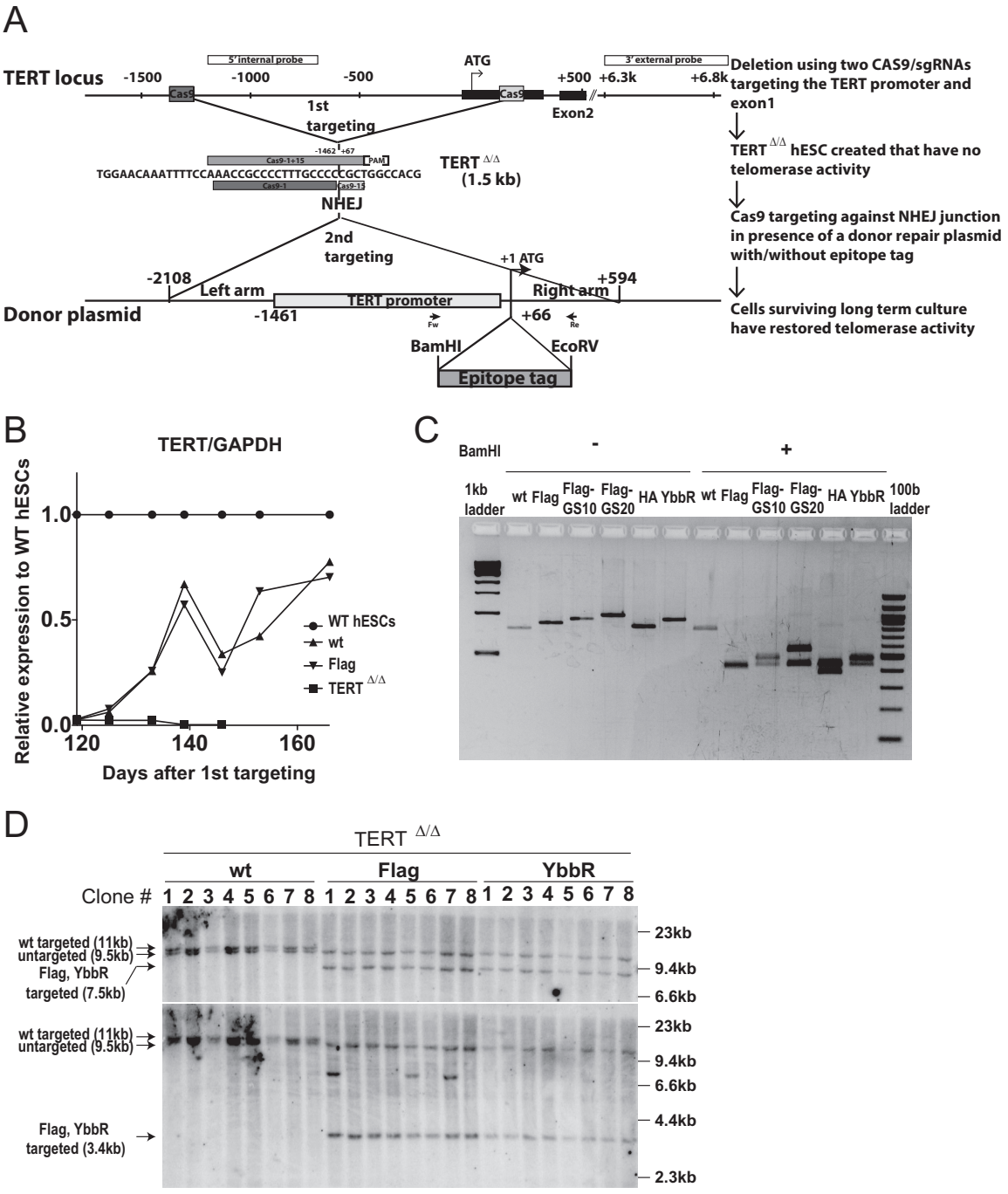

FIG 1 Generation of endogenously N-terminally tagged hESCs using scarless two-step genome editing. (A) Schematic overview of the two-step genome-editing approach used to insert epitope tags into the N terminus of endogenous TERT. First, a TERT knockout cell line (TERT$^{\Delta/\Delta}$) that lacks the region between 1.5 kb upstream and 66 bp downstream of the first ATG was established using two Cas9/sgRNAs (sg-1 and sg-15). Second, an sgRNA against the newly synthesized NHEJ-derived junction (−1462 and +67: sg1+15) was coelectroporated with donor plasmids containing the deleted regions with, or without, epitope tags after the first ATG of TERT. After the second targeting, the cells were passaged until all of the parental TERT$^{\Delta/\Delta}$ hESCs died due to telomere shortening. (B) Relative expression levels of TERT mRNA measured by quantitative RT-PCR over a time course after genome editing (day 0, first editing; day 86, second editing). Levels of expression of targeted wild-type (wt) and Flag-TERT hESCs are shown relative to those seen with nontargeted original wild-type (WT) hESCs. TERT$^{\Delta/\Delta}$ cells are plotted until the last time point before the TERT$^{\Delta/\Delta}$ cultures died. Expression of TERT was normalized to GAPDH. WT and TERT$^{\Delta/\Delta}$ cell data are identical to the data in reference 52. (C) PCR genotyping of the targeted cells after selection. Bulk DNA was used for PCR using the first ATG, and the products were digested with BamHI to confirm the insertion of epitope tags. wt, wild type. (D) Southern blot genotyping of targeted hESCs. After all TERT$^{\Delta/\Delta}$ hESCs died, single-cell-derived colonies were isolated from bulk populations. Genomic DNA was digested with BamHI and blotted using either 3′-external (top) or 5′-internal (bottom) probes. An untargeted allele appears as a 9.5-kb band. The sizes of the correctly targeted allele were 11 kb (wild type) or 7.5 kb (Flag, YbbR), respectively, for the external probe and 11 kb (wild type) or 3.4 kb (Flag, YbbR), respectively, for the internal probe.

TABLE 1 Summary of nomenclature and amino acid and DNA sequences used in this study

Nomenclature in the paper	Full name	Amino acid sequence
Flag	3×Flag	MGSDYKDHDGDYKDHDIDYKDDDDKDI
Flag-GS10	3×Flag-GS10	MGSDYKDHDGDYKDHDIDYKDDDDKDIGSGSGSGSGSGSGSGSGSGSDI
Flag-GS20	3×Flag-GS20	MGSDYKDHDGDYKDHDIDYKDDDDKDIGSGSGSGSGSGSGSGSGSGSDIGSGSGSGSGSGSGSGSGSDI
HA	HA	MGSYPYDVPDYADI
HA-GS10	HA-GS10	MGSYPYDVPDYADIGSGSGSGSGSGSGSGSGSDI
YbbR	YbbR-TEV-3×Flag	MGSDSLEFIASKLAENLYFQSASMDYKDHDGDYKDHDIDYKDDDDKDI
Halo	Halo	MGSAEIGTGFPFDPHYVEVLGERMHYVDVGPRDGTPVLFLHGNPTSSYVWRNIIPHVAPTHRCIAPDLIGMG KSDKPDLGYFFDDHVRFMDAFIEALGLEEVVLVIHDWGSALGFHWAKRNPERVKGIAFMEFIRPIPTWD EWPEFARETFQAFRTTDVGRKLIIDQNVFIEGTLPMGVVRPLTEVEMDHYREPFLNPVDREPLWRFPNE LPIAGEPANIVALVEEYMDWLHQSPVPKLLFWGTPGVLIPPAEAARLAKSLPNCKAVDIGPGLNLLQED NPDLIGSEIARWLSTLEISGDI
Halo-GS10	Halo-GS10	MGSAEIGTGFPFDPHYVEVLGERMHYVDVGPRDGTPVLFLHGNPTSSYVWRNIIPHVAPTHRCIAPDLIGMG KSDKPDLGYFFDDHVRFMDAFIEALGLEEVVLVIHDWGSALGFHWAKRNPERVKGIAFMEFIRPIPTWDE WPEFARETFQAFRTTDVGRKLIIDQNVFIEGTLPMGVVRPLTEVEMDHYREPFLNPVDREPLWRFPNELPI AGEPANIVALVEEYMDWLHQSPVPKLLFWGTPGVLIPPAEAARLAKSLPNCKAVDIGPGLNLLQEDNPD LIGSEIARWLSTLEISGDIGSGSGSGSGSGSGSGSGSGSDI
3×Flag-GS (for AAVS1 overexpression in HCT116)	3×Flag-GS	MGSDYKDHDGDYKDHDIDYKDDDDKDIGGGSGGM
3×Flag (for AAVS1 overexpression in hESCs)	3×Flag	MGSDYKDHDGDYKDHDIDYKDDDDKEFM

To test the hypothesis that these proliferation defects were due to the endogenous N-terminal tagging of TERT, we decided to systematically test the effects of the smaller epitope tags 3×Flag (abbreviated below as Flag), HA, and YbbR-TEV-3×Flag (YbbR; a label-accepting tag derived from the *ybbR* open reading frame [ORF] of the *Bacillus subtilis* genome [55]) inserted into the endogenous TERT locus (Table 1). In addition, we tested whether the addition of a flexible polypeptide linker between the Flag tag and TERT would restore TERT function. To this end, we directly compared Flag-TERT to 3×Flag-GS10 (Flag-GS10) and 3×Flag-GS20 (Flag-GS20), where GS10 and GS20 indicate linkers consisting of 10 and 20 repeats of glycine and serine, respectively (Table 1).

Each of these editing approaches in $TERT^{\Delta/\Delta}$ was successful in restoring cellular viability beyond the proliferative capacity of $TERT^{\Delta/\Delta}$. Next, single-cell-derived targeted cells were isolated and genotyped by PCR and Southern blotting (Fig. 1C and D; see also Fig. 3B and C). As expected from our previous report (52), in each case (wild type and all instances of the N-terminal TERT tagging), only one of the deleted TERT loci was restored, resulting in hemizygous $TERT^{tag/\Delta}$ cell lines (Fig. 1D).

Short telomeres associated with endogenous tagging of TERT. We analyzed TERT mRNA expression in the genetically engineered hESCs (Fig. 2A). Reverse transcriptase quantitative PCR (RT-qPCR) analysis of the targeted cells established that the levels of TERT mRNA expression in all tagged lines, with the exception of the YbbR-TERT cells, were similar to those seen with cells edited to restore the wild-type untagged TERT. In YbbR-TERT cells, TERT expression was reduced to about 40% compared to wild-type cell levels and these cells showed a slight proliferative defect that was less severe than the one seen in Halo-TERT cells. Despite this mild proliferation defect, the YbbR-TERT cells could be maintained in culture for more than 100 days and were used for further analysis. All other cell lines proliferated at a rate indistinguishable from that seen with the wild-type cells. All tagged hESCs, including YbbR-TERT cells, remained pluripotent based on the expression of the OCT4 pluripotency marker (Fig. 2A). Next, we analyzed telomerase activity in these cells. YbbR-TERT cells had a slight reduction in telomerase activity as measured using the telomeric repeat amplification protocol (TRAP) assay (Fig. 2B). We previously established that the telomerase RNA human TR (hTR), rather than TERT, is limiting for telomerase activity in wild-type hESCs and that $TERT^{+/-}$ cells do not have a 50% reduction in telomerase activity (52). This argues that the reduced TERT mRNA level in YbbR-TERT cells cannot fully account for their reduced telomerase activity. A similar reduction in activity was also evident in HA-TERT cells, despite the wild-type TERT expression in these cells. Cells expressing Flag-TERT, regard-

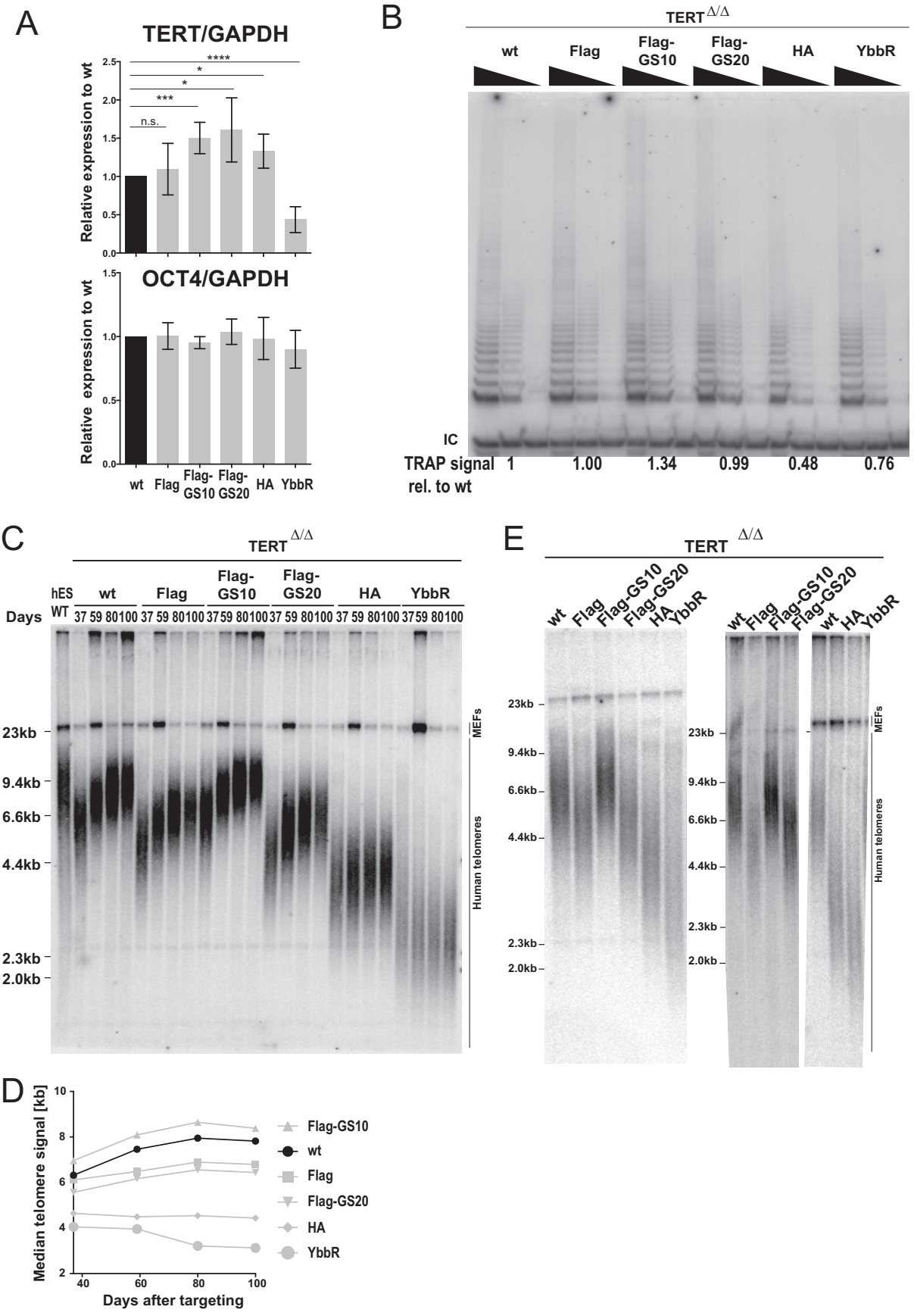
A
TERT/GAPDH
Relative expression to wt
2.5
2.0
1.5
1.0
0.5
0.0
****
*
*
***
n.s.
OCT4/GAPDH
Relative expression to wt
1.5
1.0
0.5
0.0
wt
Flag
Flag-GS10
Flag-GS20
HA
YbbR
B
TERT Δ/Δ
wt
Flag
Flag-GS10
Flag-GS20
HA
YbbR
IC
TRAP signal rel. to wt
1
1.00
1.34
0.99
0.48
0.76
C
TERT Δ/Δ
hES WT
wt
Flag
Flag-GS10
Flag-GS20
HA
YbbR
Days
37 59 80 100 37 59 80 100 37 59 80 100 37 59 80 100 37 59 80 100 37 59 80 100
23kb
9.4kb
6.6kb
4.4kb
2.3kb
2.0kb
MEFs
Human telomeres
D
Median telomere signal [kb]
10
8
6
4
2
40
60
80
100
Days after targeting
Flag-GS10
wt
Flag
Flag-GS20
HA
YbbR
E
TERT Δ/Δ
wt
Flag
Flag-GS10
Flag-GS20
HA
YbbR
23kb
9.4kb
6.6kb
4.4kb
2.3kb
2.0kb
MEFs
Human telomeres

less of the presence or size of a GS linker, had overall levels of telomerase activity equivalent to those seen with wild-type TERT cells (Fig. 2B).

To further characterize telomerase function in these endogenous locus-tagged TERT hESCs, we measured telomere length at several time points after the second editing step. Before the second editing event, which restored TERT function, telomeres were short but elongated in cells complemented with the wild-type sequence (without tag) over time back to the telomere length set point of the original hESC wild-type cells. Surprisingly, all tagged versions of TERT except Flag-GS10-TERT were unable to elongate telomeres to a length similar to that seen with isogenic wild-type TERT cells (Fig. 2C). The median telomere hybridization signal intensity in wild-type TERT cells increased from 6.3 kb to 7.8 kb over the term of 64 days. In contrast, telomeres remained stable at 4.5 kb in HA-TERT cells and at 3.5 kb in YbbR-TERT cells over the same period of time (Fig. 2D). These defects in restoring telomere length could be explained by the reduced TERT expression in YbbR-TERT cells and the reduced telomerase activity in YbbR-TERT and HA-TERT cells. However, Flag-TERT and Flag-GS20-TERT also showed a deficit in telomere elongation (Fig. 2C). Their telomeres elongated from 6.1 kb to 6.8 kb and 5.6 kb to 6.4 kb, respectively (Fig. 2D). Shorter telomeres in Flag-TERT and Flag-GS20-TERT cells cannot be simply explained by reductions of expression levels of TERT or telomerase activity as these did not differ significantly from the levels seen with isogenic wild-type edited cells (Fig. 2A).

To exclude the possibility that these shorter telomeres were artifacts of this particular genome-editing experiment, three independent experiments were performed, and they confirmed the reproducibility of shorter telomeres associated with endogenous tagging of TERT (Fig. 2E). Telomeres in Flag-GS10-TERT cells elongated to an extent similar to that seen with cells restored to wild type in these independent experiments (Fig. 2E).

Next, we analyzed the telomere length distribution of individual clones isolated after the second targeting step (Fig. 3). In wild-type TERT cells, telomeres showed some telomere length heterogeneity between clones but were on average longer than the telomeres in Flag- and YbbR-TERT cells (Fig. 3A). Flag-TERT clones 1, 5, 7, 11, 12, 13, and 15 possessed significantly shorter telomeres (Fig. 3A). On the basis of Southern blot data, these clones were aberrantly targeted at the 5′ end of TERT. Additional Southern blot genotyping using three different probes revealed that these clones had an aberrant integration of the donor plasmid backbone 5′ upstream of the right homology arm (Fig. 3B and C). Similar events have been described previously (41, 56) and are possibly the result of heterologous targeting where one side (here, the 3′ homology arm) of the double-stranded break is repaired by homology-mediated repair and the other side by nonhomologous end joining (NHEJ). Still, as shown by analysis of only correctly targeted cells, the telomeres in the Flag-TERT clones were collectively shorter than the telomeres of the wild-type TERT cell lines (Fig. 3A and D). This analysis highlights that the defect in telomere elongation is highly penetrant and is not the result of the aberrant behavior of a subset of cells.

Telomere length comparison between Flag and Flag-GS10 cells suggested that inclusion of a GS10 linker between TERT and the Flag tag could alleviate the telomere length defect. To test if this is a general feature of N-terminal tagging of TERT, we evaluated the impact of the GS10 linker in combination with the HA tag. Again,

FIG 2 Endogenous tagging of TERT disrupts telomere maintenance and results in telomere length shorter than that seen with wild-type hESCs. (A) Relative expression levels of TERT and OCT4 mRNA in the endogenously epitope-tagged hESCs compared to isogenic wt cells measured by quantitative RT-PCR. Expression levels of TERT and OCT4 were normalized to GAPDH. n.s., $P > 0.05$; *, $P < 0.05$; ***, $P < 0.001$; ****, $P < 0.0001$ (two-tailed Student's *t* test). (B) Telomeric repeat amplification protocol (TRAP) assay of whole-cell extracts from nonclonal wt, Flag, Flag-GS10, Flag-GS20, HA, and YbbR hESCs using decreasing amounts of protein (200, 40, and 8 ng). TRAP signals relative to those of wt hESCs were quantified and are shown at the bottom of the lanes (40 ng). IC, internal control. (C) Telomere restriction fragment assay of the targeted bulk population hESCs over a time course after targeting (days 37, 59, 80, and 100 after the second targeting). Restoration of telomerase after the second targeting resulted in substantial telomere elongation and an overall increase in telomere signal intensity. After digestion with MboI and AluI, 2 μg of genomic DNA was loaded in each lane and hybridized with a TTAGGG radioactive probe. (D) Quantification of median telomere length shown in panel C. (E) Telomere restriction fragment assay, as in panel C, of three independent editing experiments. Samples were collected at days 51 (left gel), 53 (middle), and 37 (right) after the second targeting.

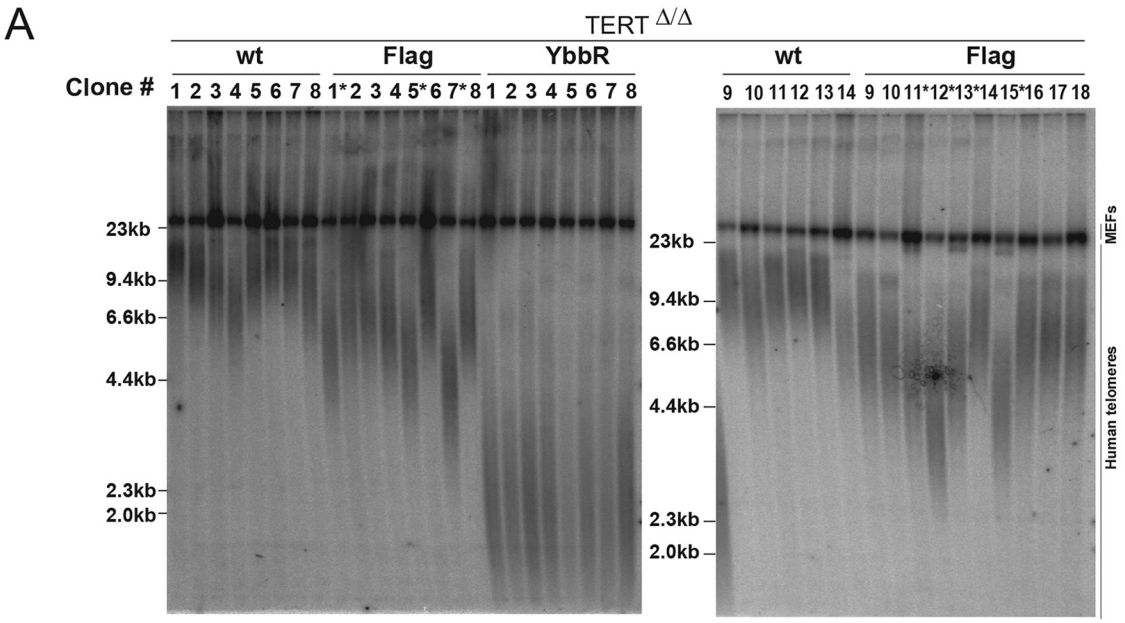
A
TERT Δ/Δ
wt
Flag
YbbR
wt
Flag
Clone # 1 2 3 4 5 6 7 8 1* 2 3 4 5* 6 7* 8 1 2 3 4 5 6 7 8
9 10 11 12 13 14 9 10 11* 12* 13* 14 15* 16 17 18
23kb
9.4kb
6.6kb
4.4kb
2.3kb
2.0kb
MEFs
Human telomeres

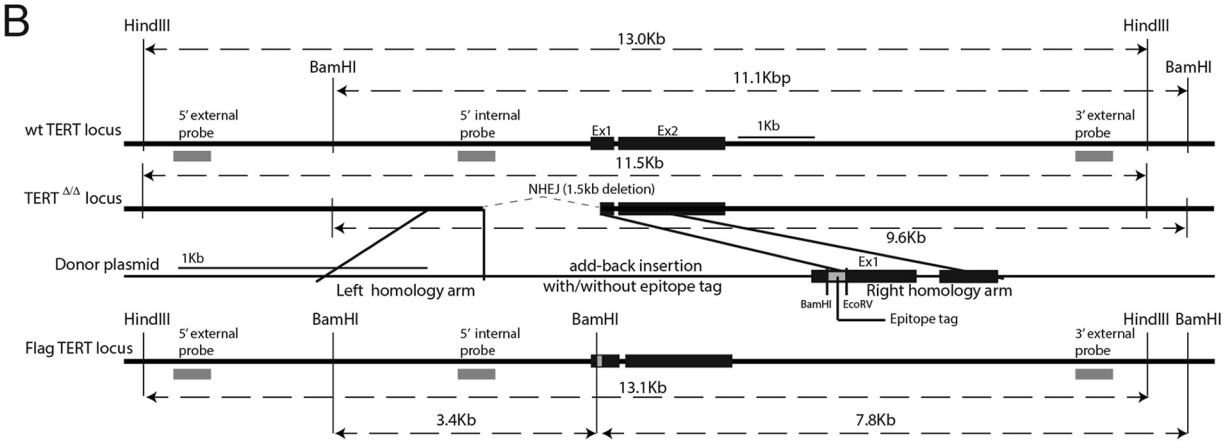
B
HindIII
BamHI
13.0Kb
11.1Kbp
wt TERT locus
5' external probe
5' internal probe
Ex1
Ex2
1Kb
3' external probe
11.5Kb
TERT Δ/Δ locus
NHEJ (1.5kb deletion)
9.6Kb
Donor plasmid
1Kb
Left homology arm
add-back insertion
with/without epitope tag
Ex1
BamHI
EcoRV
Right homology arm
Epitope tag
Flag TERT locus
13.1Kb
3.4Kb
7.8Kb

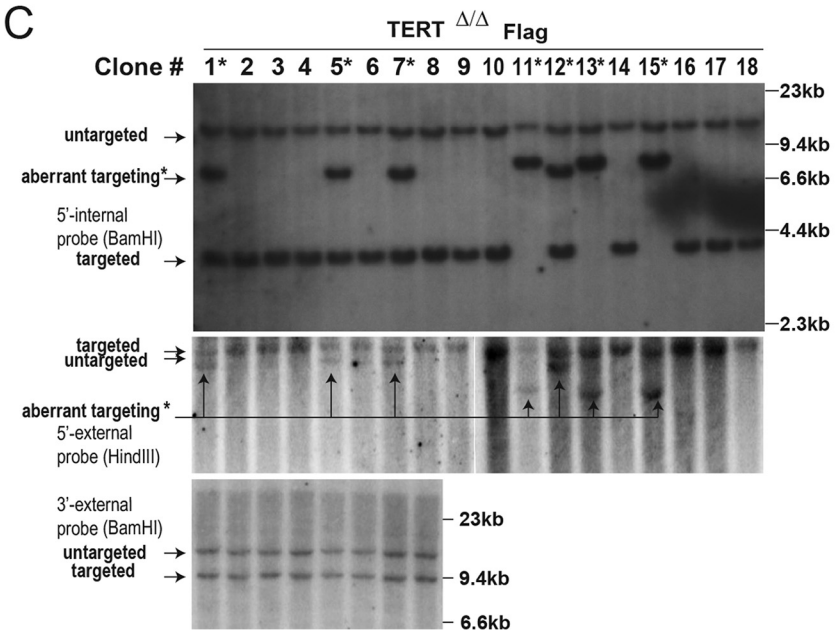
C
TERT Δ/Δ Flag
Clone # 1* 2 3 4 5* 6 7* 8 9 10 11* 12* 13* 14 15* 16 17 18
23kb
9.4kb
6.6kb
4.4kb
2.3kb
untargeted
aberrant targeting*
5'-internal probe (BamHI)
targeted
targeted untargeted
aberrant targeting *
5'-external probe (HindIII)
3'-external probe (BamHI)
untargeted
targeted
23kb
9.4kb
6.6kb

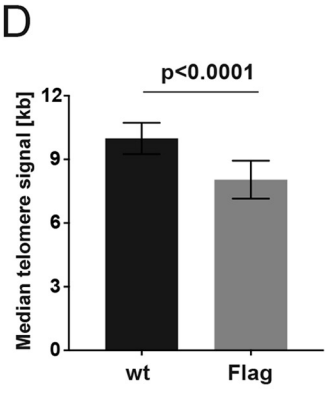
D
p<0.0001
Median telomere signal [kb]
12
9
6
3
0
wt
Flag

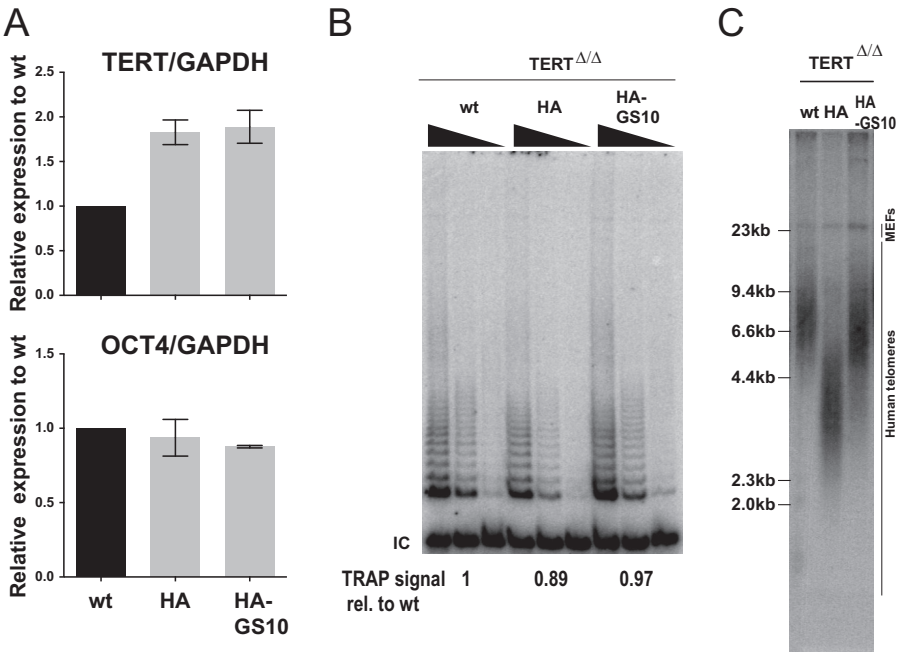

FIG 4 A GS-10 linker can alleviate defects in telomere maintenance in endogenously HA-tagged hESCs. (A) Relative expression levels of TERT and OCT4 mRNA in the endogenously epitope-tagged hESCs compared to isogenic wt cells measured by quantitative RT-PCR. Expression of TERT and OCT4 was normalized to GAPDH. HA and HA-GS10 cells whose results are shown in Fig. 2 were targeted independently. (B) Telomeric repeat amplification protocol (TRAP) assay of whole-cell extracts from nonclonal wt, HA, and HA-GS10 hESCs using decreasing amounts of protein (200, 40, and 8 ng). TRAP signals were quantified relative to wt hESCs and are shown at the bottom of the lanes. (C) Telomere restriction fragment assay of the targeted hESCs 42 days after the second targeting.

HA-TERT cells showed significant defects in telomere length maintenance, despite wild-type levels of TERT expression and telomerase activity (Fig. 2A and B and 4A and B). In contrast, HA-GS10-TERT cells had almost wild-type telomere lengths (Fig. 4C). These results indicate that the insertion of a GS10 linker can reduce defects associated with genetically tagging the TERT N terminus.

Slower telomere elongation kinetics by overexpression of Flag-TERT relative to untagged TERT. N-terminal tagging of TERT is often used as a modification to mark overexpressed TERT. Therefore, we wanted to determine whether the effects that we detected for the N-terminal tagging of TERT at its endogenous locus in hESCs are specific to the stem cell system compared to the field standard transgene-mediated TERT overexpression in cancer cell lines. To this end, we knocked out TERT ($TERT^{-/-}$) in HCT116 cells (36), a colon carcinoma cell line, using the same strategy as previously described in hESCs (18). In these $TERT^{-/-}$ cells, telomeres shorten progressively, and cells eventually die due to critically short telomeres (36). If TERT is ectopically expressed in these cells, viability and telomere maintenance are restored and telomeres elongate. We used this assay to measure the ability of variously tagged forms of TERT to elongate telomeres. We overexpressed either the wild type or 3×Flag-GS-TERT (see Table 1 for AAVS1 transgene tag sequence) driven by a CAGGS promoter from the AAVS1 locus (Fig. 5A). After insertion of these TERT overexpression constructs into the

FIG 3 Southern blot genotyping of targeted hESC clones and clonal variability of telomere length. (A) Telomere restriction fragment assay of the targeted hESCs over a time course after targeting. After digestion with MboI and AluI, 2 μg of genomic DNA was loaded into each lane and hybridized with a TTAGGG radioactive probe. Aberrantly targeted clones are marked with an asterisk. (B) Schematic overview of genotyping for N-terminal tagging at the endogenous TERT locus. Genomic DNA from single-cell-derived hESC clones was isolated and digested with either BamHI or HindIII. For genotyping, 5′-internal, 5′-external, and 3′-external probes were used. (C) Southern blot analysis for clonal Flag-TERT hESCs using three different probes. Clones 1, 5, 7, 11, 12, 13, and 15 were aberrantly targeted 5′ upstream of the right homology arm, as indicated with an asterisk. (D) Quantification of median telomere length from correctly genome edited individual clones (wt, $n = 14$; Flag, $n = 11$). $P < 0.0001$ (two-tailed Student's t test).

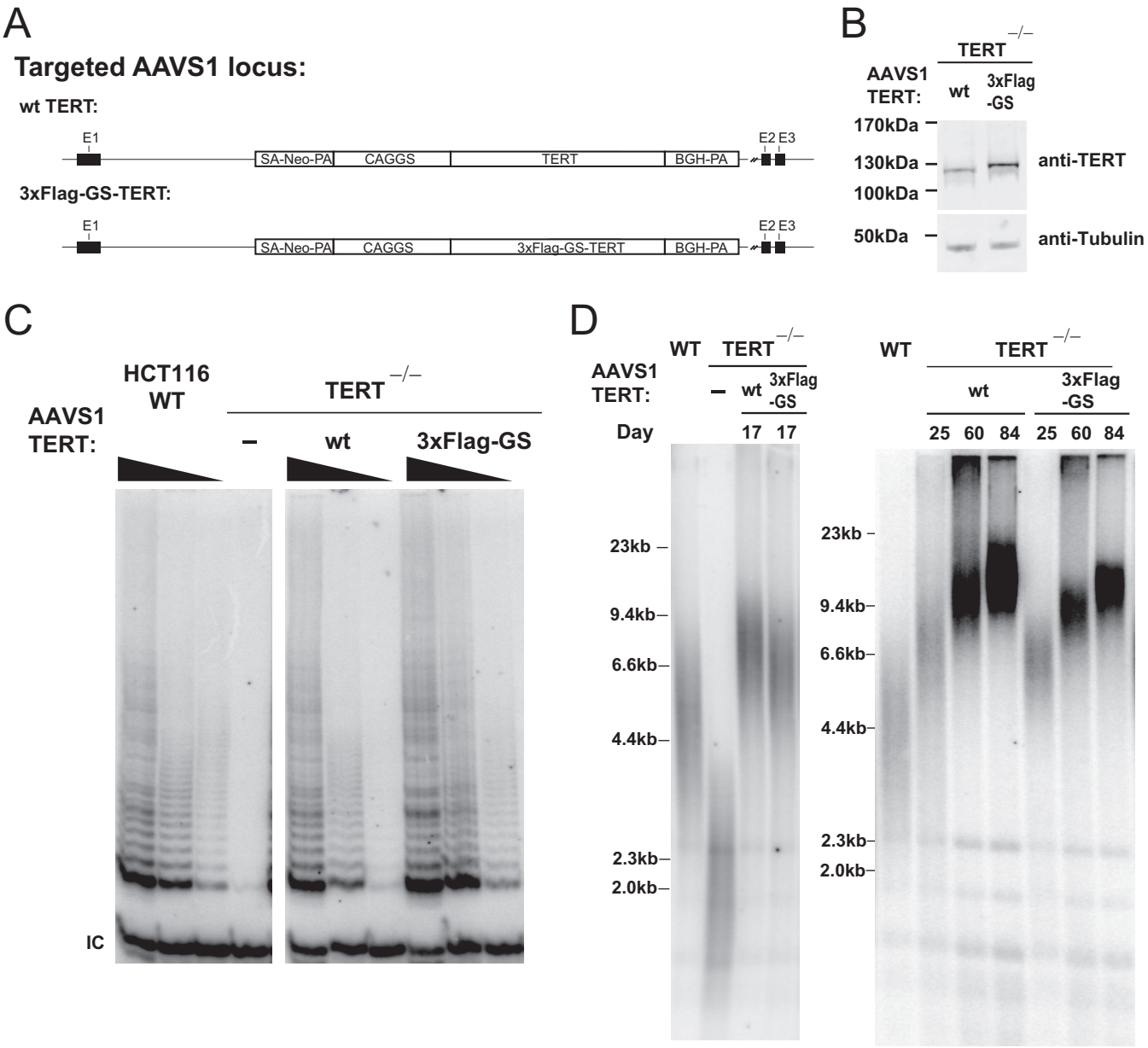

FIG 5 Overexpression of Flag-TERT in TERT$^{-/-}$ cells reveals that telomere elongation was slower than that seen with wt TERT. (A) Targeting schematic of wt or 3×Flag-GS-TERT overexpression from the AAVS1 locus in the TERT knockout (KO) HCT116 cell line (TERT$^{-/-}$). The TERT$^{-/-}$ HCT116 cell line was established by insertion of a stop codon into exon 1 of TERT using targeting vectors described previously (18). (B) Immunoblot of total TERT and tubulin protein in wt and 3×Flag-GS-TERT-overexpressing TERT$^{-/-}$ cells from whole-cell extracts. (C) TRAP assay of whole-cell extracts from parental HCT116 and TERT$^{-/-}$ cells and wt or 3×Flag-GS-TERT-overexpressing TERT$^{-/-}$ cells using protein titration (200, 40, and 8 ng). (D) Telomere restriction fragment assay of telomere elongation in TERT$^{-/-}$ cells mediated by overexpression of either wt or 3×Flag-GS-TERT at the AAVS1 locus. Data indicate the time (in days) after genome editing at the AAVS1 locus. An independent targeting experimental replicate performed for overexpression of wt and 3×Flag-GS-TERT gave the same levels of relative TRAP activity (data not shown) and telomere length differences (one replicate is shown at the left and the other replicate at the right). WT, the parental HCT116 cell line.

AAVS1 locus of TERT$^{-/-}$ cells, the telomere length gradually recovered in TERT and 3×Flag-GS-TERT cells. Yet 3×Flag-GS-TERT-overexpressing cells showed telomere elongation rates that were lower than those seen with wild-type TERT overexpression, despite 3×Flag-GS-TERT cells having greater telomerase activity and protein expression levels (Fig. 5B to D).

Next, we addressed the effects of TERT overexpression in hESCs that were Flag-TERT, YbbR-TERT, or wild type (TERT$^{wt/\Delta}$) at the endogenous locus. In these cells, we overexpressed TERT, 3×Flag-TERT, TR, or GFP from the AAVS1 locus following integration of

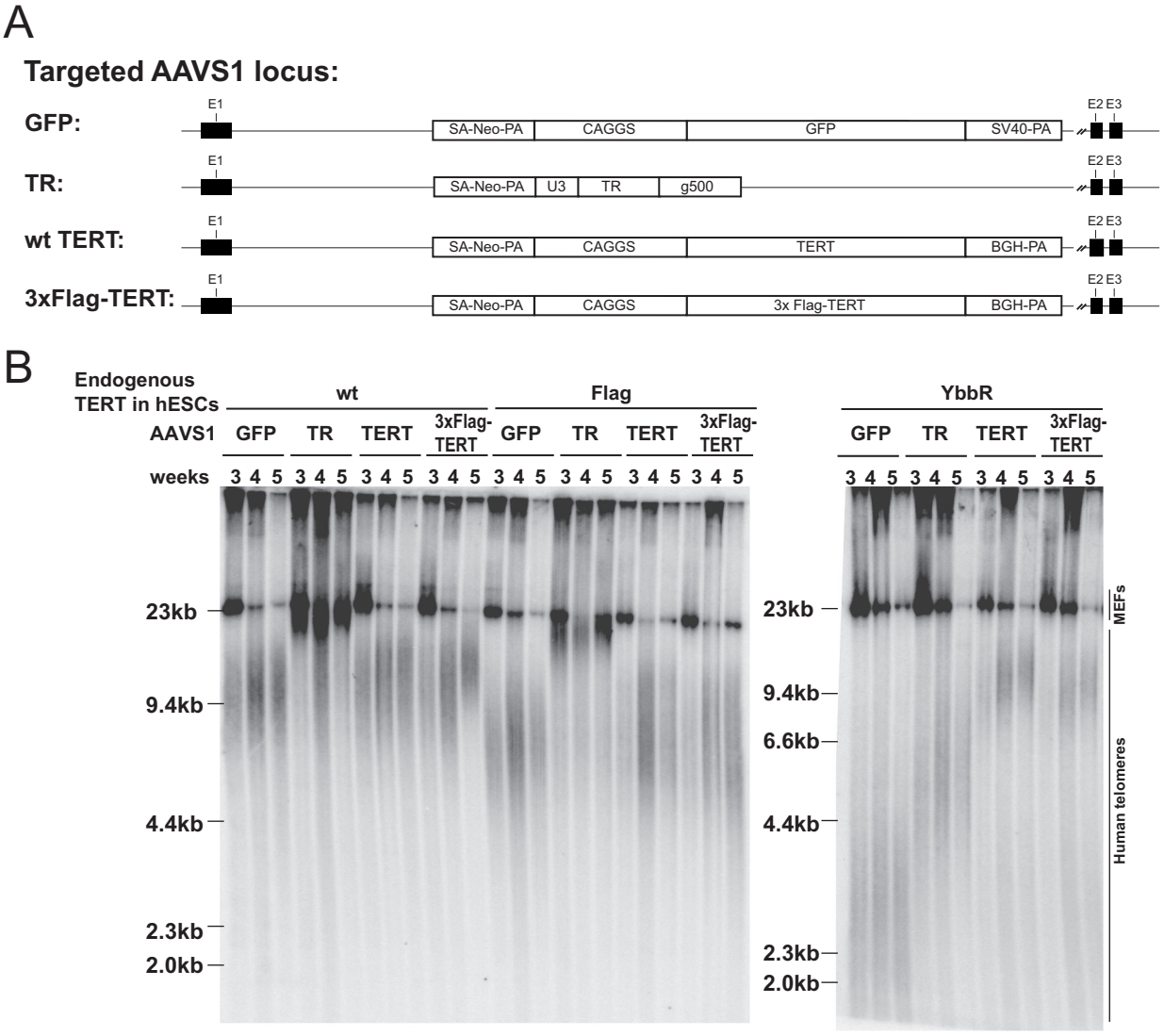

FIG 6 Overexpression of TERT and TR in tagged hESCs suggests potential postassembly defects for N-terminally tagged telomerase. (A) Targeting schematic of GFP, TR, wt TERT, or Flag-TERT overexpression from the AAVS1 locus in endogenously targeted hESCs. "g500" in the TR overexpression plasmid indicates 500 bp downstream of the genomic hTR locus. (B) Telomere restriction fragment assay of targeted wt, Flag, or YbbR hESCs overexpressing GFP, TR, wt TERT, or Flag-TERT at the AAVS1 locus. Samples were collected 3, 4, and 5 weeks (passages) after the targeting.

these by genome editing (Fig. 6A). In agreement with our previous report (52), TERT overexpression was almost neutral in hESCs, resulting in only modest telomere elongation (Fig. 6B). In contrast, TR overexpression led to dramatic telomere elongation in wild-type cells (Fig. 6B). Similarly, in endogenous-locus Flag-TERT cells, overexpression of TERT or Flag-TERT from the AAVS1 locus was largely neutral while TR overexpression led to telomere elongation (Fig. 6B). However, a strikingly inverse outcome was observed in YbbR cells. In these cells, TERT or 3×Flag-TERT overexpression resulted in pronounced telomere elongation whereas telomere elongation due to TR overexpression was blunted (Fig. 6B). These results highlight that N-terminal tagging of TERT can lead to distinct defects. In YbbR-TERT cells, TERT expression is limiting for telomerase levels. In contrast, TERT in Flag-TERT cells is not limiting and the reduced telomere elongation in these cells appears to result from a postassembly defect of telomerase RNP containing Flag-TERT. These data demonstrate that N-terminal modifications of TERT can impair telomerase function both in stem cells at a physiologically endogenous level of expression and also upon TERT overexpression in cancer cells.

N-terminal tagging of TERT results in reduced telomerase repeat addition processivity. Previous studies showed that the TEN domain of TERT plays important

roles for repeat addition processivity (RAP). We hypothesized that N-terminal tagging of TERT might disrupt RAP. To specifically test this hypothesis, we measured the processivity of endogenously tagged telomerase. We used an oligonucleotide-purification method (57) for the purification of human telomerase from genetically engineered hESCs. This purification enables enrichment of endogenous telomerase, independently of an epitope tag. Lysates from genetically engineered hESCs were incubated with the telomeric template affinity oligonucleotide beads for binding. Following serial washes, enriched telomerase was eluted from the beads using the displacement oligonucleotide, which cannot be extended by telomerase due to addition of 2′-3′-dideoxycytidine at the 3′ end. Then, the eluted fraction was assayed for telomerase activity using a direct extension assay in the presence of excess telomeric-repeat primer, which allows assaying of RAP (Fig. 7A). All N-terminally tagged telomerases tested showed reduced RAP compared to telomerase isolated from isogenic cells edited to express wild-type TERT (Fig. 7B). This result was confirmed in several independent experiments (Fig. 7C). These data suggest that shorter telomeres in the tagged cells could in part result from reduced RAP of N-terminally modified telomerases.

DISCUSSION

Key regulatory steps of telomerase involve its assembly, recruitment to, and activity at telomeres (reviewed in reference 20). Here, we report that N-terminal amino acid additions to TERT can impair telomerase function in multiple ways: TERT mRNA expression levels can be changed, and telomerase's overall activity, as well as its RAP, can be reduced (summarized in Table 2). We do not fully understand the molecular basis for all of these defects, and yet our findings allow us to draw the key conclusion that N-terminal fusions to TERT can adversely alter TERT expression and protein function, resulting in telomere maintenance at a reduced telomere length set point. These findings are important for future attempts to investigate steps of telomerase regulation and telomere length control at physiological telomerase expression levels.

On the basis of our experiments, we predict that the successful visualization of TERT in naturally telomerase-positive primary cells will be more challenging than has been previously demonstrated for HeLa and HEK293 cells (58, 59). At least in HEK293 cells, TERT tagging resulted in an approximately 8-fold-higher total TERT mRNA expression level. This could suggest that the targeting strategy used can result in an epigenetic lesion aberrantly increasing TERT expression after editing. For both cell types (HeLa and HEK293 cells), only a subset of TERT gene loci has been modified such that the tagged TERT is expressed in the presence of wild-type protein (58, 59). It is therefore possible that the residual wild-type TERT maintained telomeres in these cells, while the tagged TERT might have been predominantly TERT alone (free of hTR) or assembled into functionally compromised enzyme. It is important for future studies of active RNP localization to use an editing strategy that ensures that the visualized TERT protein is at an endogenous expression level and has endogenous TERT function in the absence of any wild-type TERT. Our findings suggest that pluripotent stem cells provide a sensitive system that can detect physiologically perturbed cellular regulation of telomere length maintenance. Due to this sensitivity, we expect that using the stem cell system will uncover novel nuances of telomerase regulation and telomere maintenance.

Our findings raise questions with regard to how to most usefully epitope tag TERT at its endogenous locus in future studies. From our comparison between HA-TERT and HA-GS10-TERT, we conclude that the addition of a flexible spacer can reduce the negative effects of TERT N-terminal tagging on telomere maintenance. However, cells edited to express the Flag-GS20-TERT allele showed a reduced telomere elongation rate compared to cells restored to the wild type, suggesting that the linker length impacts tagged TERT function. Our experiments identified Flag-GS10 and HA-GS10 as N-terminal TERT tagging modifications not deleterious for telomerase function. These tags will aid in the biochemical characterization of TERT in stem cells as well as in the

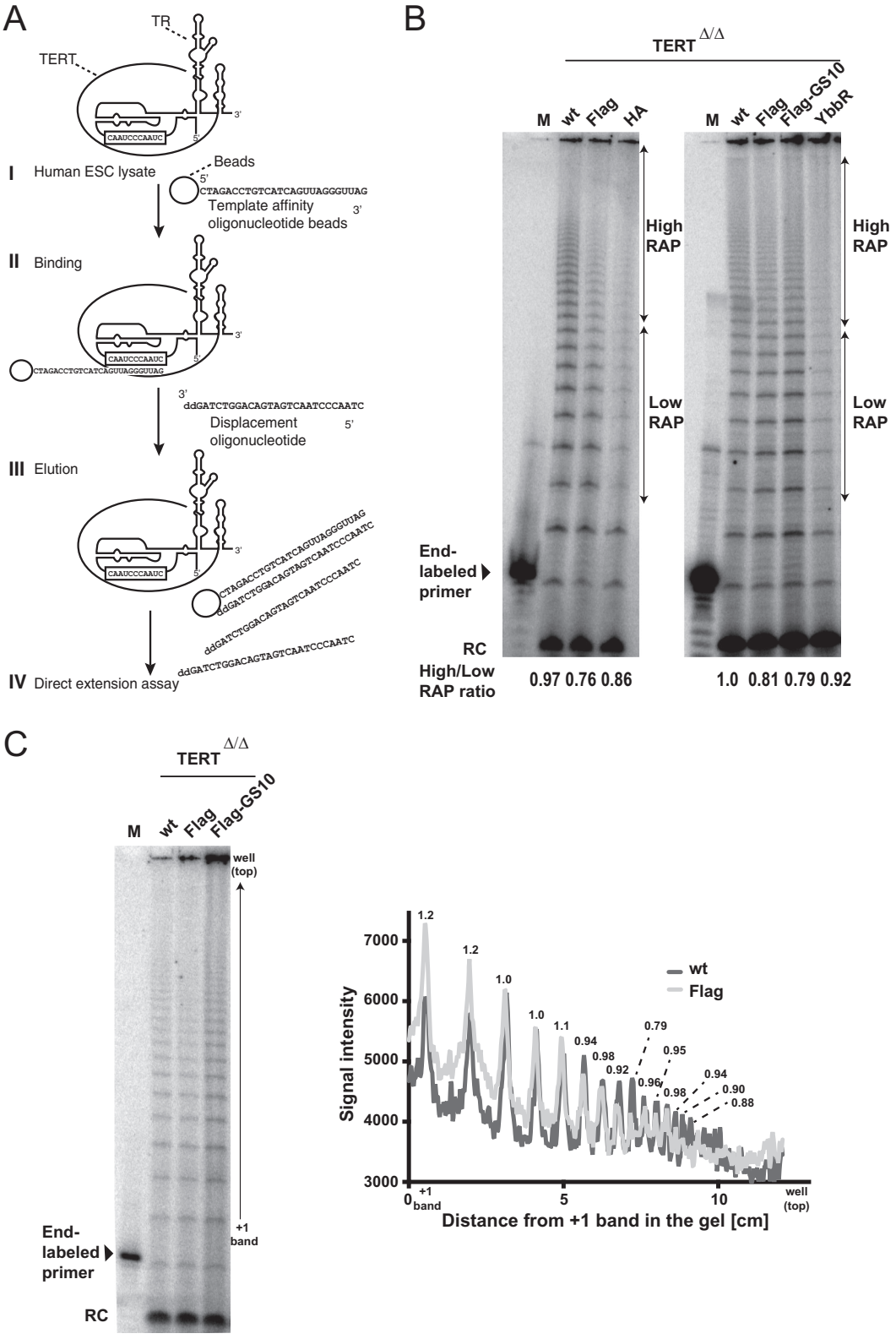

FIG 7 N-terminally tagged TERT is defective in repeat addition processivity. (A) Schematic overview of purification of endogenous telomerase by template affinity oligonucleotide purification as previously reported in reference 57. (I) Lysate form wt or tagged hESCs were prepared using hypotonic buffer. (II) The lysate was incubated with the telomerase template affinity oligonucleotide-conjugated beads. (III) After unspecific binding on the beads was washed off, enriched telomerase was eluted using the displacement oligonucleotide, which possesses a sequence complementary to the template affinity oligonucleotide but cannot be elongated by telomerase due to its 3′-end 2′-3′-dideoxycytidine. (IV) The elution fraction was used for direct telomerase activity assay. (B) Direct telomerase activity assay for wt or endogenously tagged hESCs. An 18-nt $(TTAGGG)_3$ primer

(Continued on next page)

TABLE 2 Summary of the variety of epitope tags used in this study and the phenotypes of endogenous tagging

N-tag TERT	Size of insertion (bp)	Expression	Telomerase activity	Telomere length	Repeat addition processivity
Halo-GS10	966	Lower than wt[a]	Lower than wt[a]	Shorter than wt[a]	
Flag-GS20	210	Higher than wt	wt level	Shorter than wt	
YbbR	153	Lower than wt	Lower than wt	Shorter than wt	
Flag-GS10	144	Higher than wt	~1.3-fold higher than wt	wt level	
Flag	78	wt level	wt level	Shorter than wt	Low
HA	39	Higher than wt	Lower than wt	Shorter than wt	Low

[a]Data not shown. wt, wild type.

visualization of TERT in fixed samples but do not provide a strategy for single-molecule live-cell imaging of TERT.

Previous experiments established that the linker region between the TEN domain and the remainder of TERT is dispensable for catalytic activity of telomerase (60). On that basis, we hypothesized that an insertion of Halo into this linker region could allow functional tagging of TERT. We tested this by inserting a Halo, YbbR, and Flag tag at a position between Y325 and A326 of TERT. Unfortunately, these experiments have so far been unsuccessful in generating a TERT with retained biological function (data not shown). Similarly, adding a GS10 linker between TERT and an N-terminal Halo tag (Halo-GS10 TERT hESCs) did not fully restore TERT function to the wild-type level (data not shown).

The defects in telomere elongation in Flag-TERT cells in comparison to wild-type TERT cells could be caused by recruitment defects of tagged telomerase, similarly to previously described TERT DAT mutants (47–50), in addition to the RAP impairment. Understanding the molecular basis for telomerase recruitment to and RAP at telomeres is highly relevant to telomere biology, as a subset of disease-associated mutations in TERT are specifically defective in RAP or impair recruitment (61–63). Currently, studies of these TERT mutants are limited by the need for overexpression of TERT to characterize their biochemical defects. The assay used here to characterize the RAP defects associated with tagging the N terminus of TERT is highly sensitive and can relate changes in RAP to changes in telomere length. This approach provides a system to characterize the impact of RAP defects on telomere length in an endogenous telomerase subunit expression setting.

MATERIALS AND METHODS

hESC culture. Genome-editing experiments were performed in WIBR#3 hESCs (64) (NIH stem cell registry no. 0079). Cell culture was carried out as described previously (65). hESC lines were maintained on a layer of inactivated mouse embryonic fibroblasts (MEFs) in hESC medium (Dulbecco's modified Eagle's medium–F-12 medium [DMEM–F-12; Lifetech] supplemented with 20% KnockOut serum replacement [Lifetech], 1 mM glutamine [Lifetech], 1% nonessential amino acids [Lifetech], 0.1 mM β-mercaptoethanol [Sigma], 1,000 U/ml penicillin-streptomycin [Lifetech], and 4 ng/ml fibroblast growth factor 2 [Lifetech]). Cultures were passaged every 5 to 7 days either manually or enzymatically with collagenase type IV (Lifetech) (1.5 mg/ml) and gravitational sedimentation by 3 washes in wash medium (DMEM–F-12 [Lifetech] supplemented with 5% fetal bovine serum [Lifetech] and 1,000 U/ml penicillin-streptomycin [Lifetech]).

Gene editing in hESCs. All targeting experiments were performed as previously described (39, 41). Cas9 and all sgRNAs were expressed using the pX330 plasmid (60). Endogenously tagged TERT hESC lines were generated by two targeting steps, as reported previously by Chiba et al. (52). Briefly, 1×10^7 to 2×10^7 hESCs were coelectroporated with 15 μg of two pX330 plasmids targeting bp -1418 to -1399 (AACCGCCCCTTTGCCCTAG) and bp $+110$ to $+129$ (TACCGCGAGGTGCTGCCGC) from the transcriptional

FIG 7 Legend (Continued)
was used as the substrate of the direct extension assay. This 18-nt substrate was used as an end-labeled marker. A 12-nt $(TTAGGG)_2$ primer was used as the recovery control (RC) for ethanol precipitation. Telomerase activity represented in the region indicated by arrows was quantified, and the ratio of high RAP to low RAP is shown at the bottom of the gel. (C) Direct telomerase activity assay as described for panel A. Lysates of wt and tagged TERT hESCs from panel B were prepared independently followed by telomerase template oligonucleotide purification and a direct-extension assay to measure telomerase activity. To visualize the RAP defect, the graph to the right shows the signal intensity of the gel to the left for wild-type cells with the signal intensities for Flag-TERT cells superimposed. Numbers above each peak indicate Flag/wt signal ratios.

start site and 7.5 μg of a GFP expression plasmid was electroporated along with pX330. Cells were sorted for GFP fluorescence 72 h after electroporation. Single-cell-derived hESC colonies were isolated, and their targeting was confirmed by Southern blotting and PCR, followed by sequencing. A total of 120 clones were analyzed, and three homozygously targeted hESC lines ($TERT^{\Delta/\Delta}$) were obtained. For the second targeting, pX330 plasmids were designed with sgRNAs against the newly formed NHEJ-derived junction site in $TERT^{\Delta/\Delta}$ cells and electroporated with 35 μg of a repair plasmid that carried either the deleted wild-type TERT promoter and coding element (wild type [wt]) or an insertion of an epitope tag after the first ATG of TERT (3×Flag [Flag], 3×Flag-GS10 [Flag-GS10], 3×Flag-GS20 [Flag-GS20], HA, or YbbR-TEV-3×Flag [YbbR]). After the second targeting, cells were continuously passaged. Over a period of 120 days, all $TERT^{\Delta/\Delta}$ lines that did not undergo the second targeting step died due to critically short telomeres. However, cells that were correctly targeted in the second targeting step regained TERT expression and outgrew untargeted cells. These cells were analyzed in bulk or as single-cell-derived clones, after the parental $TERT^{\Delta/\Delta}$ control culture, which did not undergo the second targeting step, had completely died. Targeting of individual clones was confirmed by Southern blotting.

Gene editing in HCT116. TERT gene disruption was performed as published previously (18). Cells were transfected with plasmids expressing zinc finger nucleases (ZFNs) targeting exon 1 of TERT, along with a donor plasmid expressing a phosphoglycerate kinase (PGK) promoter-driven hygromycin resistance cassette. Transfection was performed using Lipofectamine 3000 (Lifetech) per the instructions of the manufacturer. Targeted cells were selected using 300 μg/ml hygromycin (Thermo). $TERT^{-/-}$ clonal cells were selected and assayed for the complete loss of telomerase activity using TRAP (protocol below). AAVS1 targeting was performed as previously described (18). Cells were transfected with a plasmid expressing ZFNs to target the AAVS1 locus, along with a donor plasmid containing TERT cDNA and a splice acceptor neomycin (NEO) resistance cassette. Targeted cells were selected using 250 μg/ml G418 (Thermo).

Southern blotting and PCR genotyping. Southern blot analysis was performed as previously described (39, 65) using an external 3′ probe for TERT (bp 6280 to 6846 downstream of the TERT first ATG), an external 5′ probe (bp 5481 to 5006 upstream of the TERT first ATG), and an internal 5′ probe (bp 1813 to 1206 upstream of the TERT first ATG). Primers used for PCR genotyping are located in an internal region of the donor plasmid due to inefficient PCR amplification of GC-rich sequences (forward [Fw], GGCCGATTCGACCTCTCT; reverse [Re], CTCCTTCAGGCAGGACACCT).

qRT-PCR. RNA was extracted with TRIzol (Lifetech) and treated with DNase I (NEB). RNA (600 ng) was transcribed to cDNA with iScript reverse transcriptase (Bio-Rad) and random or poly(A) priming. Quantitative RT-PCR (qRT-PCR) was performed with Kapa SYBR fast (Kapa Biosystems) in 384-well format with a total reaction volume of 10 μl per well. A 2-μl volume of cDNA from the iScript reaction mixture was used for the detection of TERT mRNA. For measuring the expression levels of all other genes, cDNA was diluted 1:10 and 2 μl was used for qPCR. Expression levels of TERT, OCT4, and TR were normalized to expression of GAPDH (glyceraldehyde-3-phosphate dehydrogenase). Relative expression levels were calculated based on threshold cycle ($\Delta/\Delta C_T$ and/or ΔC_T) analysis. qRT-PCR primers used in this study were as follows: hTERT_qPCR_Fw (TGTCAAGGTGGATGTGACGG) and hTERT_qPCR_Rev (GAGGAGCTCTGCTCG ATGAC), hGAPDH1_qPCR_A (CAGTCTTCTGGGTGGCAGTGA) and hGAPDH1_qPCR_S (CGTGGAAGGACTCA TGACCA), OCT4_qPCR_A (CGTTGTGCATAGTCGCTGCT) and OCT4_qPCR_S (GCTCGAGAAGGATGTGGTCC), and TR_qPCR_Fw (CCCTAACTGAGAAGGGCGTA) and TR_qPCR_Rev (AGAATGAACGGTGGAAGGCG).

Detecting telomere length. To isolate genomic DNA, hESC lines were washed with phosphate-buffered saline (PBS), released from the feeder cell layer by treatment with 1 mg/ml collagenase type IV, and washed 3 times in wash media by gravitational sedimentation to minimize levels of contaminating MEF cells. Genomic DNA was then prepared as described previously (25). While this method removes the vast majority of MEFs, the signal from mouse telomeres is disproportionate to that from human telomeres as mouse telomeres are longer. Mouse telomeres are not resolved under these assay conditions and run as a band at around 23 kb (indicated on the side of the radiograph) (66). Because MEF telomeres are size resolved from human telomeres, they do not interfere with analysis of hESC telomere length. Genomic DNA was digested with MboI and AluI overnight at 37°C. The resulting DNA was normalized and run on 0.75% agarose (Seakem ME agarose; Lonza), dried under vacuum for 2 h at 50°C, denatured in 0.5 M NaOH–1.5 M NaCl for 30 min with shaking at 25°C, and neutralized with 1 M Tris (pH 6.0)–2.5 M NaCl with shaking at 25°C twice for 15 min each time. The gel was then prehybridized in Church's buffer (1% bovine serum albumin [BSA], 1 mM EDTA, 0.5 M $NaP0_4$ [pH 7.2], 7% SDS) for 1 h at 55°C before addition of a ^{32}P-end-labeled $(T_2AG_3)_3$ telomeric probe. The gel was washed 3× for 30 min each time in 4× SSC (1× SSC is 0.15 M NaCl plus 0.015 M sodium citrate) at 50°C and once for 30 min in 4× SSC–0.1% SDS at 25°C before exposure on a phosphorimager screen was performed.

Immunoblotting. After being heated to 80°C for 5 min, protein samples were cooled to room temperature and resolved by SDS-PAGE. Protein was then transferred to a nitrocellulose membrane and subsequently incubated with mouse antitubulin (DM1A; Calbiochem) (1:500) and mouse anti-TERT (56, 57, 67)–4% nonfat milk (Carnation)–TBS buffer (150 mM NaCl, 50 mM Tris [pH 7.5]) overnight at 4°C. The membrane was washed in TBS and incubated with goat anti-mouse antibody–Alexa Fluor 680 (Life Technologies) (1:2,000)–4% nonfat milk–TBS for 1 h at room temperature. After extensive washing with TBS, the membrane was visualized on a Li-COR Odyssey imager (68).

Assaying telomerase catalytic activity. The PCR-based telomeric repeat amplification protocol (TRAP) assay was performed as previously described using TS (AATCCGTCGAGCAGAGTT) and ACX (GCGCGGCTTACCCTTACCCTTACCCTAACC) for amplification of telomeric repeats and TSNT (AATCCGTC GAGCAGAGTTAAAAGGCCGAGAAGCGAT) and NT (ATCGCTTCTCGGCCTTTT) as an internal control. Cell extracts were generated by repeated freeze-thaw cycles in hypotonic lysis buffer (HLB) (20 mM HEPES,

2 mM $MgCl_2$, 0.2 mM EGTA, 10% glycerol, 1 mM dithiothreitol [DTT], 0.1 mM phenylmethylsulfonyl fluoride [PMSF]) supplemented with 0.5% CHAPS {3-[(3-cholamidopropyl)-dimethylammonio]-1-propanesulfonate}. Protein concentrations were measured using a Bradford protein assay kit (Bio-Rad).

For enrichment of endogenous telomerase, lysates from hESCs were incubated with 10 μl of streptavidin-agarose resin (Sigma-Aldrich) conjugated with 5′ biotinylated telomeric template oligonucleotide (CTAGACCTGTCATCAGUUAGGGUUAG; the underlined nucleotides represent 2′-*O*-methyl RNA) (69). The resin and lysate were incubated at room temperature for 2 h. The resin was washed three times with HLB supplemented with 150 mM NaCl–0.1% NP-40. Purified telomerase was eluted by the use of 10 μl of the elution buffer (HLB supplemented with 150 mM NaCl, 0.1% NP-40, and a 30 μM concentration of the displacement oligonucleotide [CTAACCCTAACTGATGACAGGTCTAG with a 2′,3′-dideoxyguanosine modification at the 3′ terminus]) for 1 h at room temperature. The resin was removed using Empty Micro Spin columns (Harvard Apparatus). A primer extension assay using oligonucleotide-purified telomerase was performed in a 20-μl reaction mixture containing 8 μl of the eluate fraction, a 500 nM concentration of the telomeric primer [$(T_2AG_3)_3$] in MTB buffer (50 mM Tris acetate, 3 mM $MgCl_2$, 50 mM potassium acetate, 1 mM EGTA, 1 mM spermidine, 5 mM β-mercaptoethanol) with 250 μM dTTP and dATP, 5 μM dGTP, and 2 μl of anti-[^{32}P]dGTP (Perkin-Elmer) (3,000 Ci/mmol, 10 mCi/ml). The reaction mixture was incubated at 30°C for 40 min, and then the reaction was stopped by adding 80 μl of TES buffer (50 mM Tris [pH 7.5], 20 mM EDTA, 0.2% SDS). After phenol-chloroform extraction and ethanol precipitation, the extension products were resolved on a 10.5% polyacrylamide–7 M urea–0.6× Tris-borate-EDTA gel. As a recovery control, end-radiolabeled $(T_2AG_3)_2$ primer was added before ethanol precipitation, and end-radiolabeled $(T_2AG_3)_3$ primer was loaded as a size marker. Dried gels were visualized using a Typhoon phosphorimager.

ACKNOWLEDGMENTS

We thank Kartoosh Heydari for technical assistance and the Collins and Hockemeyer laboratories for helpful discussion.

K. Collins, J. M. Vogan, and X. Zhang are supported by US National Institutes of Health grant R01-HL079585. R. A. Wu and K. Collins were supported by NIH RO1-GM054198. K. Chiba is supported by a Nakajima foundation fellowship. D. Hockemeyer is a New Scholar in Aging of the Ellison Medical Foundation and a Pew-Stewart Scholar in the Cancer Research. The work in the Hockemeyer laboratory is supported by the Glenn Foundation, the Shurl and Kay Curci Foundations, the Siebel Stem Cell Center, and NIH R01-CA196884.

K. Chiba conducted the experiments in hESCs. J. M. Vogan and X. Zhang conducted all experiments in HCT116 cells. K. Chiba and R. A. Wu conducted the oligonucleotide-based telomerase purification and direct extension assays. M. S. Gill prepared several DNA constructs. K. Collins and D. Hockemeyer supervised research. K. Collins and D. Hockemeyer wrote the manuscript with the assistance of all other authors.

REFERENCES

1. Greider CW, Blackburn EH. 1985. Identification of a specific telomere terminal transferase activity in Tetrahymena extracts. Cell 43:405–413. https://doi.org/10.1016/0092-8674(85)90170-9.
2. Blackburn EH, Greider CW, Szostak JW. 2006. Telomeres and telomerase: the path from maize, Tetrahymena and yeast to human cancer and aging. Nat Med 12:1133–1138. https://doi.org/10.1038/nm1006-1133.
3. Armanios M, Blackburn EH. 2012. The telomere syndromes. Nat Rev Genet 13:693–704. https://doi.org/10.1038/nrg3246.
4. Kim NW, Piatyszek MA, Prowse KR, Harley CB, West MD, Ho PL, Coviello GM, Wright WE, Weinrich SL, Shay JW. 1994. Specific association of human telomerase activity with immortal cells and cancer. Science 266:2011–2015. https://doi.org/10.1126/science.7605428.
5. Cohen SB, Graham ME, Lovrecz GO, Bache N, Robinson PJ, Reddel RR. 2007. Protein composition of catalytically active human telomerase from immortal cells. Science 315:1850–1853. https://doi.org/10.1126/science.1138596.
6. Yi X, Shay JW, Wright WE. 2001. Quantitation of telomerase components and hTERT mRNA splicing patterns in immortal human cells. Nucleic Acids Res 29:4818–4825. https://doi.org/10.1093/nar/29.23.4818.
7. Xi L, Cech TR. 2014. Inventory of telomerase components in human cells reveals multiple subpopulations of hTR and hTERT. Nucleic Acids Res 42:8565–8577. https://doi.org/10.1093/nar/gku560.
8. Ducrest AL, Szutorisz H, Lingner J, Nabholz M. 2002. Regulation of the human telomerase reverse transcriptase gene. Oncogene 21:541–552. https://doi.org/10.1038/sj.onc.1205081.
9. Podlevsky JD, Chen JJ. 2012. It all comes together at the ends: telomerase structure, function, and biogenesis. Mutat Res 730:3–11. https://doi.org/10.1016/j.mrfmmm.2011.11.002.
10. Doksani Y, de Lange T. 2014. The role of double-strand break repair pathways at functional and dysfunctional telomeres. Cold Spring Harb Perspect Biol 6:a016576. https://doi.org/10.1101/cshperspect.a016576.
11. Nandakumar J, Bell CF, Weidenfeld I, Zaug AJ, Leinwand LA, Cech TR. 2012. The TEL patch of telomere protein TPP1 mediates telomerase recruitment and processivity. Nature 492:285–289. https://doi.org/10.1038/nature11648.
12. Zhong FL, Batista LF, Freund A, Pech MF, Venteicher AS, Artandi SE. 2012. TPP1 OB-fold domain controls telomere maintenance by recruiting telomerase to chromosome ends. Cell 150:481–494. https://doi.org/10.1016/j.cell.2012.07.012.
13. Abreu E, Aritonovska E, Reichenbach P, Cristofari G, Culp B, Terns RM, Lingner J, Terns MP. 2010. TIN2-tethered TPP1 recruits human telomerase to telomeres in vivo. Mol Cell Biol 30:2971–2982. https://doi.org/10.1128/MCB.00240-10.
14. Tejera AM, Stagno d'Alcontres M, Thanasoula M, Marion RM, Martinez P, Liao C, Flores JM, Tarsounas M, Blasco MA. 2010. TPP1 is required for TERT recruitment, telomere elongation during nuclear reprogramming, and normal skin development in mice. Dev Cell 18:775–789. https://doi.org/10.1016/j.devcel.2010.03.011.
15. Wang F, Lei M. 2011. Human telomere POT1-TPP1 complex and its role in telomerase activity regulation. Methods Mol Biol 735:173–187. https://doi.org/10.1007/978-1-61779-092-8_17.
16. Wang F, Podell ER, Zaug AJ, Yang Y, Baciu P, Cech TR, Lei M. 2007. The

POT1-TPP1 telomere complex is a telomerase processivity factor. Nature 445:506–510. https://doi.org/10.1038/nature05454.
17. Xin H, Liu D, Wan M, Safari A, Kim H, Sun W, O'Connor MS, Songyang Z. 2007. TPP1 is a homologue of ciliate TEBP-beta and interacts with POT1 to recruit telomerase. Nature 445:559–562. https://doi.org/10.1038/nature05469.
18. Sexton AN, Regalado SG, Lai CS, Cost GJ, O'Neil CM, Urnov FD, Gregory PD, Jaenisch R, Collins K, Hockemeyer D. 2014. Genetic and molecular identification of three human TPP1 functions in telomerase action: recruitment, activation, and homeostasis set point regulation. Genes Dev 28:1885–1899. https://doi.org/10.1101/gad.246819.114.
19. Schmidt JC, Dalby AB, Cech TR. 2014. Identification of human TERT elements necessary for telomerase recruitment to telomeres. Elife 3:e03563. https://doi.org/10.7554/eLife.03563.
20. Hockemeyer D, Collins K. 2015. Control of telomerase action at human telomeres. Nat Struct Mol Biol 22:848–852. https://doi.org/10.1038/nsmb.3083.
21. Schmidt JC, Cech TR. 2015. Human telomerase: biogenesis, trafficking, recruitment, and activation. Genes Dev 29:1095–1105. https://doi.org/10.1101/gad.263863.115.
22. Ye JZ, Donigian JR, van Overbeek M, Loayza D, Luo Y, Krutchinsky AN, Chait BT, de Lange T. 2004. TIN2 binds TRF1 and TRF2 simultaneously and stabilizes the TRF2 complex on telomeres. J Biol Chem 279:47264–47271. https://doi.org/10.1074/jbc.M409047200.
23. Liu D, Safari A, O'Connor MS, Chan DW, Laegeler A, Qin J, Songyang Z. 2004. PTOP interacts with POT1 and regulates its localization to telomeres. Nat Cell Biol 6:673–680. https://doi.org/10.1038/ncb1142.
24. Ye JZ, Hockemeyer D, Krutchinsky AN, Loayza D, Hooper SM, Chait BT, de Lange T. 2004. POT1-interacting protein PIP1: a telomere length regulator that recruits POT1 to the TIN2/TRF1 complex. Genes Dev 18:1649–1654. https://doi.org/10.1101/gad.1215404.
25. Hockemeyer D, Sfeir AJ, Shay JW, Wright WE, de Lange T. 2005. POT1 protects telomeres from a transient DNA damage response and determines how human chromosomes end. EMBO J 24:2667–2678. https://doi.org/10.1038/sj.emboj.7600733.
26. Smogorzewska A, van Steensel B, Bianchi A, Oelmann S, Schaefer MR, Schnapp G, de Lange T. 2000. Control of human telomere length by TRF1 and TRF2. Mol Cell Biol 20:1659–1668. https://doi.org/10.1128/MCB.20.5.1659-1668.2000.
27. van Steensel B, de Lange T. 1997. Control of telomere length by the human telomeric protein TRF1. Nature 385:740–743. https://doi.org/10.1038/385740a0.
28. Loayza D, De Lange T. 2003. POT1 as a terminal transducer of TRF1 telomere length control. Nature 423:1013–1018. https://doi.org/10.1038/nature01688.
29. Kim SH, Kaminker P, Campisi J. 1999. TIN2, a new regulator of telomere length in human cells. Nat Genet 23:405–412. https://doi.org/10.1038/70508.
30. Greider CW. 2016. Regulating telomere length from the inside out: the replication fork model. Genes Dev 30:1483–1491. https://doi.org/10.1101/gad.280578.116.
31. Cristofari G, Lingner J. 2006. Telomere length homeostasis requires that telomerase levels are limiting. EMBO J 25:565–574. https://doi.org/10.1038/sj.emboj.7600952.
32. Cristofari G, Adolf E, Reichenbach P, Sikora K, Terns RM, Terns MP, Lingner J. 2007. Human telomerase RNA accumulation in Cajal bodies facilitates telomerase recruitment to telomeres and telomere elongation. Mol Cell 27:882–889. https://doi.org/10.1016/j.molcel.2007.07.020.
33. Stern JL, Zyner KG, Pickett HA, Cohen SB, Bryan TM. 2012. Telomerase recruitment requires both TCAB1 and Cajal bodies independently. Mol Cell Biol 32:2384–2395. https://doi.org/10.1128/MCB.00379-12.
34. Chen Y, Deng Z, Jiang S, Hu Q, Liu H, Songyang Z, Ma W, Chen S, Zhao Y. 2015. Human cells lacking coilin and Cajal bodies are proficient in telomerase assembly, trafficking and telomere maintenance. Nucleic Acids Res 43:385–395. https://doi.org/10.1093/nar/gku1277.
35. Tomlinson RL, Li J, Culp BR, Terns RM, Terns MP. 2010. A Cajal body-independent pathway for telomerase trafficking in mice. Exp Cell Res 316:2797–2809. https://doi.org/10.1016/j.yexcr.2010.07.001.
36. Vogan JM, Zhang X, Youmans DT, Regalado SG, Johnson JZ, Hockemeyer D, Collins K. 2016. Minimized human telomerase maintains telomeres and resolves endogenous roles of H/ACA proteins, TCAB1, and Cajal bodies. Elife 5:e18221. https://doi.org/10.7554/eLife.18221.
37. Hockemeyer D, Jaenisch R. 2016. Induced pluripotent stem cells meet genome editing. Cell Stem Cell 18:573–586. https://doi.org/10.1016/j.stem.2016.04.013.
38. Soldner F, Laganiere J, Cheng AW, Hockemeyer D, Gao Q, Alagappan R, Khurana V, Golbe LI, Myers RH, Lindquist S, Zhang L, Guschin D, Fong LK, Vu BJ, Meng X, Urnov FD, Rebar EJ, Gregory PD, Zhang HS, Jaenisch R. 2011. Generation of isogenic pluripotent stem cells differing exclusively at two early onset Parkinson point mutations. Cell 146:318–331. https://doi.org/10.1016/j.cell.2011.06.019.
39. Hockemeyer D, Wang H, Kiani S, Lai CS, Gao Q, Cassady JP, Cost GJ, Zhang L, Santiago Y, Miller JC, Zeitler B, Cherone JM, Meng X, Hinkley SJ, Rebar EJ, Gregory PD, Urnov FD, Jaenisch R. 2011. Genetic engineering of human pluripotent cells using TALE nucleases. Nat Biotechnol 29:731–734. https://doi.org/10.1038/nbt.1927.
40. Hockemeyer D, Jaenisch R. 2010. Gene targeting in human pluripotent cells. Cold Spring Harbor Symp Quant Biol 75:201–209. https://doi.org/10.1101/sqb.2010.75.021.
41. Hockemeyer D, Soldner F, Beard C, Gao Q, Mitalipova M, DeKelver RC, Katibah GE, Amora R, Boydston EA, Zeitler B, Meng X, Miller JC, Zhang L, Rebar EJ, Gregory PD, Urnov FD, Jaenisch R. 2009. Efficient targeting of expressed and silent genes in human ESCs and iPSCs using zinc-finger nucleases. Nat Biotechnol 27:851–857. https://doi.org/10.1038/nbt.1562.
42. Thomson JA, Itskovitz-Eldor J, Shapiro SS, Waknitz MA, Swiergiel JJ, Marshall VS, Jones JM. 1998. Embryonic stem cell lines derived from human blastocysts. Science 282:1145–1147. https://doi.org/10.1126/science.282.5391.1145.
43. Takahashi K, Tanabe K, Ohnuki M, Narita M, Ichisaka T, Tomoda K, Yamanaka S. 2007. Induction of pluripotent stem cells from adult human fibroblasts by defined factors. Cell 131:861–872. https://doi.org/10.1016/j.cell.2007.11.019.
44. Batista LF, Artandi SE. 2013. Understanding telomere diseases through analysis of patient-derived iPS cells. Curr Opin Genet Dev 23:526–533. https://doi.org/10.1016/j.gde.2013.07.006.
45. Batista LF, Pech MF, Zhong FL, Nguyen HN, Xie KT, Zaug AJ, Crary SM, Choi J, Sebastiano V, Cherry A, Giri N, Wernig M, Alter BP, Cech TR, Savage SA, Reijo Pera RA, Artandi SE. 2011. Telomere shortening and loss of self-renewal in dyskeratosis congenita induced pluripotent stem cells. Nature 474:399–402. https://doi.org/10.1038/nature10084.
46. Agarwal S, Loh Y-H, McLoughlin EM, Huang J, Park I-H, Miller JD, Huo H, Okuka M, Dos Reis RM, Loewer S, Ng H-H, Keefe DL, Goldman FD, Klingelhutz AJ, Liu L, Daley GQ. 2010. Telomere elongation in induced pluripotent stem cells from dyskeratosis congenita patients. Nature 464:292–296. https://doi.org/10.1038/nature08792.
47. Counter CM, Hahn WC, Wei WY, Caddle SD, Beijersbergen RL, Lansdorp PM, Sedivy JM, Weinberg RA. 1998. Dissociation among in vitro telomerase activity, telomere maintenance, and cellular immortalization. Proc Natl Acad Sci U S A 95:14723–14728. https://doi.org/10.1073/pnas.95.25.14723.
48. Armbruster BN, Banik SSR, Guo C, Smith AC, Counter CM. 2001. N-terminal domains of the human telomerase catalytic subunit required for enzyme activity in vivo. Mol Cell Biol 21:7775–7786. https://doi.org/10.1128/MCB.21.22.7775-7786.2001.
49. Armbruster BN, Linardic CM, Veldman T, Bansal NP, Downie DL, Counter CM. 2004. Rescue of an hTERT mutant defective in telomere elongation by fusion with hPot1. Mol Cell Biol 24:3552–3561. https://doi.org/10.1128/MCB.24.8.3552-3561.2004.
50. Banik SSR, Guo C, Smith AC, Margolis SS, Richardson DA, Tirado CA, Counter CM. 2002. C-terminal regions of the human telomerase catalytic subunit essential for in vivo enzyme activity. Mol Cell Biol 22:6234–6246. https://doi.org/10.1128/MCB.22.17.6234-6246.2002.
51. Greider CW. 1991. Telomerase is processive. Mol Cell Biol 11:4572–4580. https://doi.org/10.1128/MCB.11.9.4572.
52. Chiba K, Johnson JZ, Vogan JM, Wagner T, Boyle JM, Hockemeyer D. 2015. Cancer-associated TERT promoter mutations abrogate telomerase silencing. Elife 4:e07918. https://doi.org/10.7554/eLife.07918.
53. Heidenreich B, Rachakonda PS, Hemminki K, Kumar R. 2014. TERT promoter mutations in cancer development. Curr Opin Genet Dev 24:30–37. https://doi.org/10.1016/j.gde.2013.11.005.
54. Los GV, Encell LP, McDougall MG, Hartzell DD, Karassina N, Zimprich C, Wood MG, Learish R, Ohana RF, Urh M, Simpson D, Mendez J, Zimmerman K, Otto P, Vidugiris G, Zhu J, Darzins A, Klaubert DH, Bulleit RF, Wood KV. 2008. HaloTag: a novel protein labeling technology for cell imaging and protein analysis. ACS Chem Biol 3:373–382. https://doi.org/10.1021/cb800025k.
55. Yin J, Straight PD, McLoughlin SM, Zhou Z, Lin AJ, Golan DE, Kelleher NL,

Kolter R, Walsh CT. 2005. Genetically encoded short peptide tag for versatile protein labeling by Sfp phosphopantetheinyl transferase. Proc Natl Acad Sci U S A 102:15815–15820. https://doi.org/10.1073/pnas.0507705102.
56. Rouet P, Smih F, Jasin M. 1994. Introduction of double-strand breaks into the genome of mouse cells by expression of a rare-cutting endonuclease. Mol Cell Biol 14:8096–8106. https://doi.org/10.1128/MCB.14.12.8096.
57. Wu RA, Dagdas YS, Yilmaz ST, Yildiz A, Collins K. 2015. Single-molecule imaging of telomerase reverse transcriptase in human telomerase holoenzyme and minimal RNP complexes. Elife 4:e08363. https://doi.org/10.7554/eLife.08363.
58. Xi L, Schmidt JC, Zaug AJ, Ascarrunz DR, Cech TR. 2015. A novel two-step genome editing strategy with CRISPR-Cas9 provides new insights into telomerase action and TERT gene expression. Genome Biol 16:231. https://doi.org/10.1186/s13059-015-0791-1.
59. Schmidt JC, Zaug AJ, Cech TR. 2016. Live cell imaging reveals the dynamics of telomerase recruitment to telomeres. Cell 166:1188–1197.e1189. https://doi.org/10.1016/j.cell.2016.07.033.
60. Cong L, Ran FA, Cox D, Lin S, Barretto R, Habib N, Hsu PD, Wu X, Jiang W, Marraffini LA, Zhang F. 2013. Multiplex genome engineering using CRISPR/Cas systems. Science 339:819–823. https://doi.org/10.1126/science.1231143.
61. Gramatges MM, Qi X, Sasa GS, Chen JJ, Bertuch AA. 2013. A homozygous telomerase T-motif variant resulting in markedly reduced repeat addition processivity in siblings with Hoyeraal Hreidarsson syndrome. Blood 121:3586–3593. https://doi.org/10.1182/blood-2012-08-447755.
62. Zaug AJ, Crary SM, Jesse Fioravanti M, Campbell K, Cech TR. 2013. Many disease-associated variants of hTERT retain high telomerase enzymatic activity. Nucleic Acids Res 41:8969–8978. https://doi.org/10.1093/nar/gkt653.
63. Robart AR, Collins K. 2010. Investigation of human telomerase holoenzyme assembly, activity, and processivity using disease-linked subunit variants. J Biol Chem 285:4375–4386. https://doi.org/10.1074/jbc.M109.088575.
64. Lengner CJ, Gimelbrant AA, Erwin JA, Cheng AW, Guenther MG, Welstead GG, Alagappan R, Frampton GM, Xu P, Muffat J, Santagata S, Powers D, Barrett CB, Young RA, Lee JT, Jaenisch R, Mitalipova M. 2010. Derivation of pre-X inactivation human embryonic stem cells under physiological oxygen concentrations. Cell 141:872–883. https://doi.org/10.1016/j.cell.2010.04.010.
65. Soldner F, Hockemeyer D, Beard C, Gao Q, Bell GW, Cook EG, Hargus G, Blak A, Cooper O, Mitalipova M, Isacson O, Jaenisch R. 2009. Parkinson's disease patient-derived induced pluripotent stem cells free of viral reprogramming factors. Cell 136:964–977. https://doi.org/10.1016/j.cell.2009.02.013.
66. Kipling D, Cooke HJ. 1990. Hypervariable ultra-long telomeres in mice. Nature 347:400–402. https://doi.org/10.1038/347400a0.
67. Rouet P, Smih F, Jasin M. 1994. Expression of a site-specific endonuclease stimulates homologous recombination in mammalian cells. Proc Natl Acad Sci U S A 91:6064–6068. https://doi.org/10.1073/pnas.91.13.6064.
68. Fu D, Collins K. 2003. Distinct biogenesis pathways for human telomerase RNA and H/ACA small nucleolar RNAs. Mol Cell 11:1361–1372. https://doi.org/10.1016/S1097-2765(03)00196-5.
69. Schnapp G, Rodi HP, Rettig WJ, Schnapp A, Damm K. 1998. One-step affinity purification protocol for human telomerase. Nucleic Acids Res 26:3311–3313. https://doi.org/10.1093/nar/26.13.3311.